Int. J. Electrochem. Sci., 15 **(2020)** 1529 – 1538, doi: 10.20964/2020.02.60

International Journal of
ELECTROCHEMICAL
SCIENCE
www.electrochemsci.org

High Performance Lithium-Sulfur Batteries Obtained by Employing Spiked Carbon Nanofibers as Host Materials

Jiaofei Huo[1], *Yinwei Wang*[2, 3,*]

[1] Department of Mechanical and Electrical Technology, Xijing University, Xi'an 710123, China
[2] Intelligent Manufacturing Research and Development Center, Xijing University, Xi'an 710123, Chia
[3] School of Mechanical Engineering, Xijing University, Xi'an 710123, China
[*]E-mail: yinweiwang@aliyun.com

Received: 17 October 2019 / *Accepted:* 5 December 2019 / *Published:* 31 December 2019

Carbon materials have been considered as the most promising host materials for the sulfur in the past decades. Various carbon materials, including graphene, carbon sphere, carbon nanotube, prepared via different methods have been reported in the references, to improve the electrochemical performance of the lithium-sulfur batteries. In this paper, carbon nanofibers are first synthesized by electrospinning method. The as-prepared carbon nanofibers appear spiked carbon structure, which surface consists of branches. Due to the unique spiked club shape structure, the as-prepared carbon nanofiber sulfur composites display superior electrochemical activity with high specific capacity and long cycle performance. The initial specific capacity of the carbon nanofiber sulfur composites is as high as 1208 mAh/g. The capacity retention of the carbon nanofiber sulfur composites is 92% at 1C after 200 cycles.

Keywords: New Energy, Energy Storage System, Li-S Battery, Electric Vehicle, Cycle Stability

1. INTRODUCTION

Energy storage systems with high energy density and specific capacity are extremely significant for the application of electric vehicles and mobile electric devices [1, 2]. There are various energy storage systems reported in the literatures and newspapers, such as lithium-ion batteries [3], lithium-sulfur batteries [4], lithium-air batteries [5], metal-air batteries [6], supercapacitors [7]. The above energy storage systems have been researched by the researchers for many decades. Great achievements are obtained during the past decades. Especially, lithium-sulfur batteries are the hottest topic due to their high specific capacity (1675mAh/g) and energy density (2600 Wh/kg) [8, 9]. The main reason is that the element sulfur is abundant and friendly to the environment. Therefore, the lithium-sulfur batteries, which used element sulfur as cathode and lithium as anode, may become the

next generation new energy storage system for the various electric devices [10, 11].

However, there are still some issues that limit the practical employment of the lithium-sulfur batteries [12]. On the one hand, the element sulfur is electronic insulator, which is hard to transport the electronics during the electrochemical process [13]. On the other hand, some products at discharge state will dissolved into the electrolyte, which could lead to severe capacity loss and poor cycle stability [14-16]. This two main reasons cause poor electrochemical performance of the lithium-sulfur batteries. As a result, the key issues are dealing with two disadvantages at the same time [17]. In the past decades, many strategies have been used to modify the electrochemical performance of the lithium-sulfur batteries. Great amounts works are devoted to prepare suitable cathode host materials for element sulfur [18]. More recently, metal oxides are developed as host materials for the lithium-sulfur batteries, such as MnO_2 [19], TiO_2 [20], and SiO_2 [21]. However, these metal oxides are high weight in the sulfur-based composites, which lead to low energy density of lithium-sulfur batteries. Therefore, the most efficient method is still used carbon materials, which has superior conductivity and high specific surface area.

In our work, the spiked carbon nanofibers are successfully prepared and designed as host materials for sulfur. The as-prepared carbon nanofiber sulfur composites (CNF-S) possess high electronic conductivity due to their 3D nanofiber structure. Besides, the branches on the surface of the carbon nanofiber could provide adsorption for the discharge products soluble polysulfide. Combined the advantages of high electronic conductivity and adsorption for the polysulfide, the specific capacity and cycle performance of the lithium-sulfur batteries are greatly improved during the electrochemical cycles.

2. EXPERIMENTAL

2.1. Preparation of spiked carbon nanofiber

First, 1.6 g polyacrylonitrile and 1.2 g polystryrene were added into the 20 ml DMF solution and stirred for 30 min. Then, 4 ml tetrahydrofuran was added dropwise into the above mixture while stirring. The solution was electrospinning at voltage of 15 kV between needle and the collector. The resulting polymer membrane was heated at 300 ℃ for 4 h at N_2 atmosphere. As a result, the spiked carbon nanofibers were successfully prepared.

2.2. Preparation of carbon nanofiber sulfur composites

The carbon nanofiber composites were prepared via heat method at different temperature. First, the carbon nanofiber and sulfur are mixed and ground with ratio of 1:3. In detail, the mass of the spiked carbon and sulfur are 0.5 g and 1.5 g, respectively. Then, the mixture was heated at 155℃ for 12h and 300℃ for 2h. The heat process is conducted under Ar atmosphere. After cooling to room temperature, the resultant was collected and named as CNF-S composites.

2.3. Materials Characterization

The morphologies of the as-prepared samples were tested by scanning electron microscope (SEM, EVO 18) and transmission electron microscope (TEM, Tecnai F20). The crystal structure of the samples was conducted via an X-ray diffractometer (XRD, D8 Advance, BRUKER). X-ray photoelectron spectroscopy (XPS) was used to judge the chemical valence of the as-prepared samples on a Thermo ESCALAB 250Xi in an ultra-high vacuum. Raman spectra were collected with a LabRAM HR800 with the range from 100 to 3500 cm^{-1}.

2.4. Electrochemical Measurements

The electrode slurry was prepared by mixing the active materials, super P and PVDF with weight ratio of 92:2:6. NMP was used as solvent to prepare the electrode slurry. Then, the electrode slurry was uniformly coated on the Al film and dried at 60℃ for 24h. The dried electrode film was punched into circle electrode with a diameter of 15 mm. The electrochemical performance was tested by using CR2032 coin battery. In the coin battery, the as-prepared CNF-S electrode is used as cathode. A lithium film was used as the anode. The electrolyte consists of 1M LITFSI with DOL:DME=1:1. The discharge and charge profiles are obtained on LANDCT2001A between 1.8 and 2.8V. Electrochemical impedance spectra is tested on electrochemistry station CHI660E.

3. RESULTS AND DISSCUSSION

The carbon nanofibers were prepared by electrospinning method. As shown in Figure 1, the as-prepared mixture solution was placed into a syringe and fixed on a platform. The voltage between platform and collector is 15 KV. The distance is about 16 cm with a flow rate of 0.6 mL h^{-1}. The Al film is used for collecting the nanofibers film. The resultant fibrous film was dried for overnight in vacuum at 60 °C to remove the DMF. After that, the fibrous film was heated at 300 ℃ for 4 h in a N_2 atmosphere to obtain spiked club carbon nanofiber.

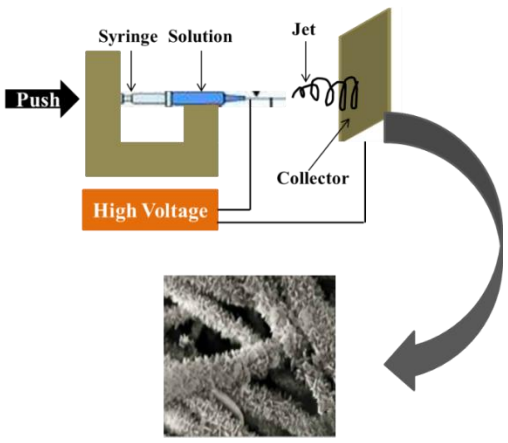

Figure 1. Preparation of the spiked carbon nanofibers.

Figure 2 a displays the morphology of the carbon nanofibers. It can be observed that the as-prepared carbon nanofibers show spiked carbon nanostructure with dimeter of 100 nm. The SEM image of the carbon nanofiber sulfur composites is displayed in Figure 2b. The element sulfur is uniformly distributed in the spiked club carbon nanofiber structure, which proves the successful preparation of CNF-S composites. The overall morphology of CNF-S composites shows similar shape comparing with the pristine carbon nanofibers. Figure 2c shows the TEM image of the CNF-S composites. It can be seen that the dimeter of the CNF-S composites is between 100 and 110 nm [22]. The surface of the CNF-S composites consists of many branches, which is beneficial for the transport of electronics as cathode materials for energy storage systems. To further demonstrate the distribution of sulfur in the carbon nanofiber structure, EDS was conducted. As shown in Figure 2d-f, the corresponding elemental mapping confirms the presence of the elements C and S in the CNF-S composites.

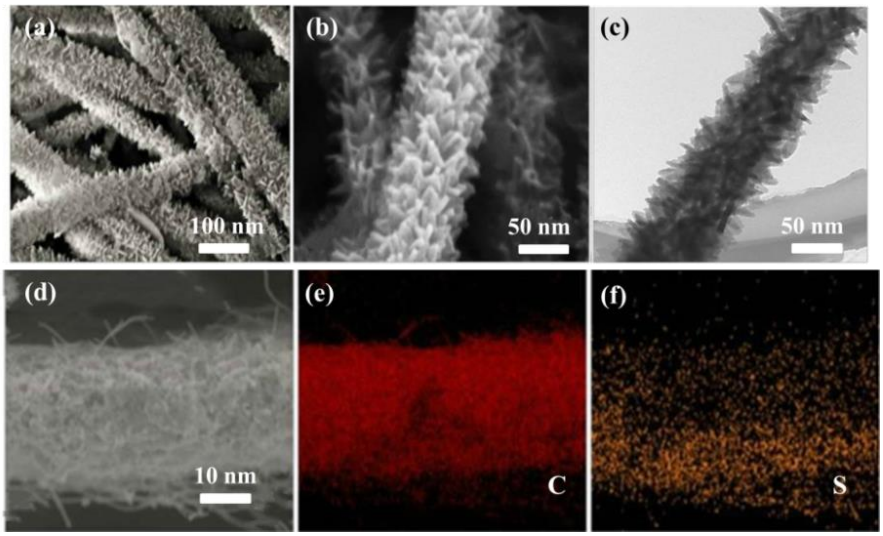

Figure 2. (a) SEM image of carbon nanofiber. (b) SEM image of carbon nanofiber sulfur composites. (c) TEM image of carbon nanofiber sulfur composites. (d-f) The corresponding elemental mapping of carbon nanofiber sulfur composites.

Figure 3a shows the XRD patterns of the carbon nanofiber, sulfur and CNF-S composites. The as-prepared carbon nanofiber exhibits typical carbon diffraction peaks. The element sulfur exhibits monoclinic structure, demonstrating typical diffraction peaks of sulfur. After heating with sulfur, the as-prepared CNF-S composites have similar diffraction peaks with the pristine sulfur, confirming the preparation of CNF-S composites. The peaks intensity of the CNF-S composites is weaker than the pristine sulfur. As described in Figure 3b, for CNF and CNF-S composites, the characteristic peaks D and G peaks are observed simultaneously, except for the position of the D and G peaks [23]. This suggests that the element sulfur was fully immersed into the carbon nanofibers. The successful immerse for the sulfur into the spiked carbon nanofiber could ensure the uniformity of the whole composites, which is beneficial for the storage of electrochemical capacity during the electrochemical

process. In all, these materials characterizations confirm the preparation of the CNF-S composites via electrospinning and heating method.

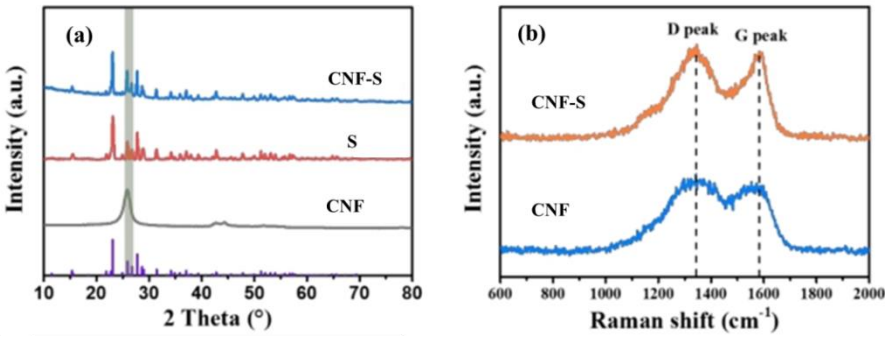

Figure 3. (a) XRD pattern of carbon nanofiber, sulfur and carbon nanofiber sulfur composites. (b) Raman spectra of carbon nanofiber and carbon nanofiber sulfur composites.

To determine the pore structure and size of the CNF and CNF-S composites, pore distribution of the samples were tested. As shown in Figure 4a, the pore size of the spiked club carbon nanofibers is about 10 nm with pore volume of 0.2 cm^3/g. While for the CNF-S composites, the pore size decreases to 6 nm with pore volume of 0.15 cm^3/g. This indicates that the pores of the carbon nanofibers have been occupied with element sulfur. As we all known, the typical mesoporous structure could promote the sulfur dipping into the mesopores, which can store sufficient sulfur and release capacity via chemical reactions. Figure 4b exhibits the XPS of C 1s for the CNF and CNF-S composites. For the pristine carbon nanofibers, the diffraction peaks at 284.5 eV and 286.1 eV are corresponding to the C=C and C-C bonds [24]. This result is consistent with the other reports. The CNF-S composites show another diffraction peak located at 288.6 eV, which is ascribed to the presence of C-S bond in the CNF-S composites.

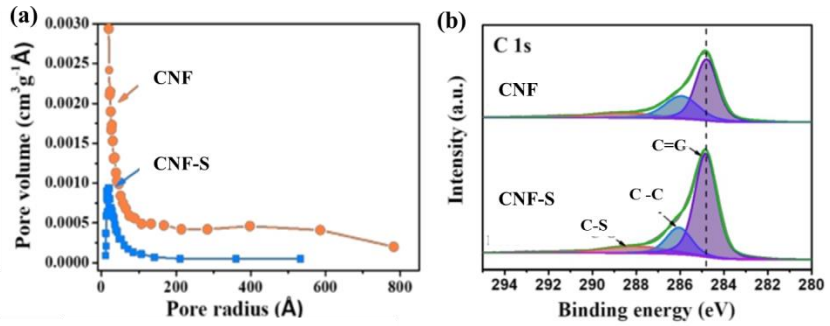

Figure 4. (a) Pore distribution of carbon nanofiber and carbon nanofiber sulfur composites. (b) XPS of C 1s spectra for carbon nanofiber and carbon nanofiber composites.

Benefiting from the perfect nanofiber structure of the CNF-S composites, the CNF-S

composites show high electrochemical performance when designed as cathode materials for the lithium-sulfur batteries. As shown in Figure 5a, it can be seen that the initial specific capacity value of the CNF-S composites reaches 1208 mAh/g at the current density of 0.05 C. However, for the pure sulfur electrode, the initial specific capacity is only 1056 mAh/g at 0.05 C. It can be also obtained from the DC curves of CNF-S composites that there are two voltage platforms at 2.3 V and 2.1 V, respectively. For the pure sulfur electrode, the voltage platforms are lower than the CNF-S composite cathode, which is caused due to the poor electronic conductivity of the sulfur. Moreover, after several electrochemical cycles, the electrolyte was adsorbed by using pure sulfur and CNF-S composites. As depicted in Figure 5b, it can be observed that the CNF-S composites show superior adsorption ability for the electrolyte, confirming the inhibiting effect for the polysulfide [25].

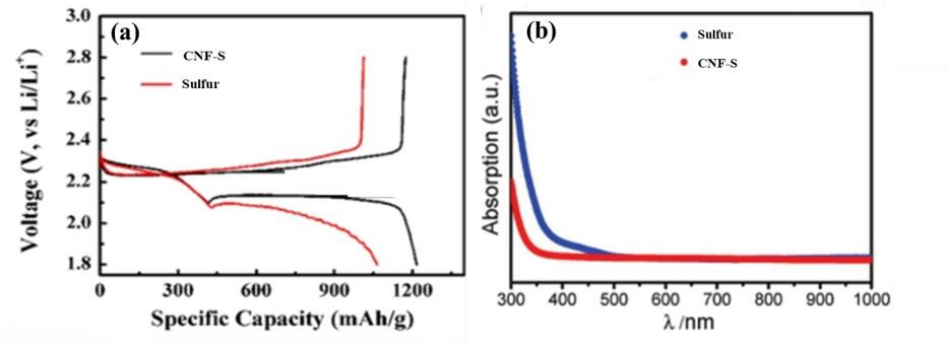

Figure 5. (a) DC curves of pure sulfur and carbon nanofiber sulfur composites. (b) UV–visible absorption spectra of the electrolyte by using sulfur and carbon nanofiber sulfur composites.

CV curves are used to judge the electrochemical reaction mechanism for the lithium-sulfur batteries, as shown in Figure 6. Figure 6a shows the CV curves of pure sulfur electrode at different scan rates. It can be observed two reduction peaks and one oxidation peak are located at 2.3 V, 2.1 V and 2.5V. They are related to the transformation from sulfur to high polysulfide and Li_2S, and finally to element sulfur. Besides, the peaks are reduced with the increase of the scan rates. For the CNF-S composites (Figure 6b), it shows similar CV shape with the pure sulfur electrode. The peak currents are much higher than the pure sulfur electrode, demonstrating high electronic conductivity. This is consistent with the DC curves (Figure 5a). From the CV results, it can be concluded that the as-preapred CNF-S composites have more superior reversibility during the scanning at constant scan rate. Especially, for the as-prepared CNF-S composite electrode, the as-prepared CNF-S electrode shows excellent electrochemical reaction kinetics, demonstrating great reversibility [26, 27]. Moreover, the CNF-S electrode exhibits higher current rate during the scan in the CV curves, confirming the superior electronic conductivity [28]. The high electronic conductivity is further proved by EIS results in the Figure 7b.

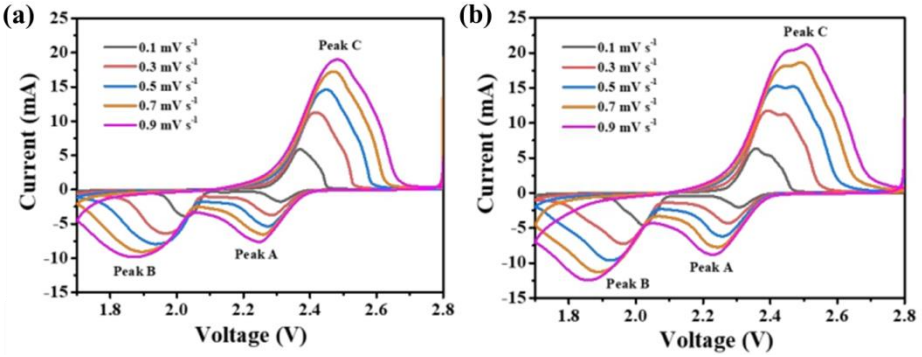

Figure 6. (a) and (b) CV curves of pure sulfur and carbon nanofiber sulfur composites at various scan rates from 0.1 mV s^{-1} to 0.9 mV s^{-1}.

Rate performance is another important electrochemical performance for the lithium-sulfur batteries. Rate capability is mainly related to the electronic conductivity and the ability for transporting the electronics [29]. To investigate the rate performance, various current densities were tested for the pure sulfur electrode and CNF-S composite electrode. As shown in Figure 7a, the capacity values at various current densities from 0.1 C to 2 C are tested for pure sulfur electrode and CNF-S composites electrode. The as-prepared CNF-S composites exhibit high capacities even at high current density of 1C and 2 C. Finally, the capacity could recover back to initial capacity value when the current densities were back to 0.1 C. However, for the pure sulfur electrode, the capacity values are fading rapidly with the increase of the current densities, demonstrating bad rate performance. Figure 7b shows the EIS of the sulfur and CNF-S composites electrodes. The semicircle in the high frequency represents charge transfer impedance, and the line in the low frequency is related to the lithium-ion duffusion [29]. It can be clearly observed that the CNF-S composites exhibit superior electronic and lithium-ion conductivity.

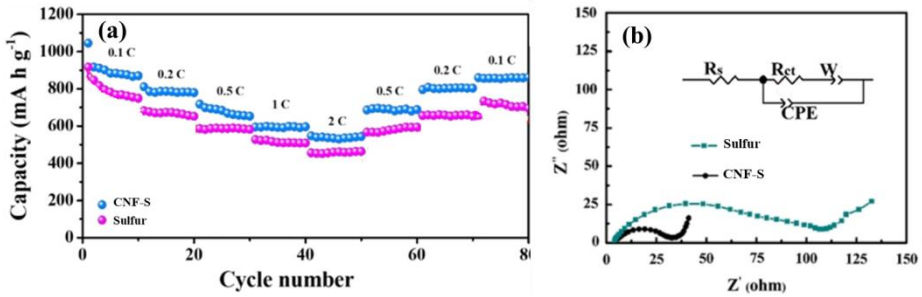

Figure 7. (a) Rate performance of pure sulfur and carbon nanofiber sulfur composites. (b) Electrochemical impedance spectra of pure sulfur and carbon nanofiber sulfur composites.

Figure 8a displays the long cycle performance of the CNF-S composites at 1 C and 2 C, respectively. The capacity of the CNF-S composites still remains 826 mAh/g with a capacity retention of 92% after 200 cycles. Even at high current density of 2 C, the capacity retention is as high as 82% after 200 cycles. This is attributed to the superior adsorption ability of CNF-S composites. To further

confirm this phenomenon, Figure 8b exhibits the photographs of the color change before and after using sulfur and carbon nanofiber sulfur composites. It can be clearly observed that the color pristine electrolyte becomes colorless after adding CNF-S composites. However, for the employment of pure sulfur, there is no color change. From this, it can be seen that the as-prepared CNF-S composites could adsorb the soluble polysulfide and inhibit the shuttle effect. Thus, the electrochemical performance can be enhanced by using the as-prepared CNF-S composite electrode. The pure sulfur electrode fails to inhibits the polysulfide migration during the electrochemical reactions.

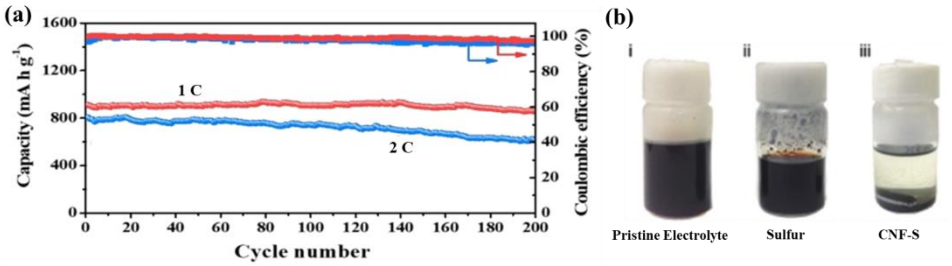

Figure 8. (a) The long cycle stability for the CNF-S composites at the current density of 1 C and 2 C, respectively. (b) Photographs of the color change before and after using sulfur and carbon nanofiber sulfur composites.

Table 1 was made for comparing the electrochemical performance of the various kinds of cathode materials for the lithium-sulfur batteries. As shown inTable1, it can be clearly observed that the as-prepared CNF-S composite electrode displays higher specific capacity than pther reported similar cathode materials. More importantly, the as-prepared CNF-S composite electrodes have more excellent cycle stability during the electrochemical cycles. The high capacity retention of 92 % can be reached after 200 cycles even at the high current density of 1C.

Table 1. Comparison of the similar cathode materials for the lithium-sulfur batteries.

Electrode	Initial Capacity	Cycle Performance	Ref
PCNF-S	954 (mAh g^{-1})	83% (200 cycles)	30
ANHCNFs	920 (mAh g^{-1})	90% (200 cycles)	31
S/HPCNF	1016 (mAh g^{-1})	80% (200 cycles)	32
HCNF	1090 (mAh g^{-1})	55% (100 cycles)	33
CNF-S	1208 (mAh g^{-1})	92% (200 cycles)	This Work

4. CONCLUSIONS

In summary, we developed spiked carbon nanofiber materials via electrospinning method. After that, the carbon nanofiber sulfur composites were successfully synthesized by heating method at different temperature. The as-prepared CNF-S composites show high specific capacity and superior cycle stability. The initial specific capacity of CNF-S composites is nearly 1208 mAh/g. Even at the

high current density of 1C, the capacity retention of the CNF-S composites remains at 92 % after 200 cycles. The high electrochemical performance is ascribed to the perfect spiked structure, which could improve the electronic conductivity. Moreover, the branches on the surface of the carbon nanofiber are beneficial for inhibiting the migration of the soluble polysulfide from the cathode sided to the anode side.

ACKNOWLEDGEMENT
We thank the support from Department of Mechanical and Electrical Technology and Intelligent Manufacturing Research and Development Center.

References

1. W. Zhang, J. F. Zhang, Y. Zhao and X. Wang, *Mater. Lett.,* 255 (2019) 126595.
2. S. P. Li, X. Chen, F. Hu, R. Zeng, Y. H. Huang, L. X. Yuan and J. Xie, *Electrochim. Acta*, 304 (2019) 11.
3. S. S. Yao, H. Tang, M. Q. Liu, L. L. Chen, M. X. Jing, X. Q. Shen, T. B. Li and J. L. Tan, *J. Alloy Compd.,* 788 (2019) 639.
4. Y. Y. Liang, N. P. Deng, J. G. Ju, X. H. Zhou, J. Yan, C. L. Zhong, W. M. Kang and B. W. Cheng, *Electrochim. Acta*, 281 (2018) 257.
5. J. Li, Y. Guo, P. Wen, J. H. Zhu, Z. G. Liu and Y. J. Qiu, *J. Electroanal. Chem*., 823 (2018) 287.
6. Y. Li, J. D. Zhu, R. W. Shi, M. Dirican, P. Zhu, C. Y. Yan, H. Jia, J. Zang, J. H. He and X. W. Zhang, *Chem. Eng. J.*, 349 (2018) 376.
7. D. C. An, L. Shen, D. N. Lei, L. H. Wang, H. Ye, B. H. Li, F. Y. Kang and Y. B. He, *J. Energ. Chem.*, 31 (2019) 19.
8. W. M. Kang, L. L. Fan, N. P. Deng, H. J. Zhao, Q. X. Li, M. Naebe, J. Yan, and B. W. Cheng, *Chem. Eng. J*., 333 (2018) 185.
9. X. Song, S. Q. Wang, G. P. Chen, T. Gao, Y. Bao, L. X. Ding and H. H. Wang, *Chem. Eng. J*., 333 (2018) 564.
10. X. Song, T. Gao, S. Q. Wang, Y. Bao, G. P. Chen, L. X. Ding and H. H. Wang, *J. Power Sources*, 356 (2017) 172.
11. Z. J. Liu, B. L. Liu, P. Q. Guo, X. N. Shang, M. Z. Lv, D. Q. Liu and D. Y. He, *Electrochim. Acta*, 269 (2018) 180.
12. X. Y. Li, N. P. Fu, J. Z. Zou, X. R. Zeng, Y. M. Chen, L. M. Zhou and H. T. Huang, *Mater. Lett*., 209 (2017) 505.
13. X. H. Zhao, M. Kim, Y. Liu, H. J. Ahn, K. W. Kim, K. K. Cho and J. H. Ahn, *Carbon*, 128 (2018) 138.
14. N. P. Deng, W. M. Kang, J. G. Ju, L. L. Fan, X. P. Zhuang, X. M. Ma, H. S. He, Y. X. Zhoa dn B. W. Cheng, *J. Power Sources*, 346 (2017) 1.
15. J. H. Zhu, R. Pitcheri, T. Kang, Y. Guo, J. Li and Y. J. Qiu, *Ceram. Int*., 44 (2018) 16837.
16. S. Q. Li, J. Warzywoda, S. Wang, G. F. Ren, Z. Y. Fan, *Carbon*, 124 (2017) 212.
17. Z. H. Wang, X. D. Wang, W. Sun and K. N. Sun, *Electrochim. Acta*, 252 (2017) 127.
18. Z. A. Zhang, G. C. Wang, Y. Q. Lai and J. Li, *J. Alloy Compd*., 663 (2016) 501.
19. J. G. Wang, Y. Yang and F. Y. Kang, *Electrochim. Acta*, 168 (2015) 271.
20. Q. Li, Z. A. Zhnag, K. Zhang, J. Fang, Y. Q. Lai and J. Li, *J. Power Sources*, 256 (2014) 137.
21. Y. H. Wu, M. X. Gao, X. Li, Y. F. Liu and H. G. Pan, *J. Alloy Compd*., 608 (2014) 220.
22. L. Zhou, X. J. Lin, T. Huang and A. S. Yu, *Electrochim. Acta*, 116 (2014) 210.
23. J. F. Zhang, G. R. Li, Y. G. Zhang, W. Zhang, X. Wang, Y. Zhao, J. D. Li and Z. W. Chen, *Nano Energ*., 64 (2019) 103905.

24. Z. X. Jian, H. L. Li, R. Cao, H. L. Zhou, H. Z. Xu, G. J. Zhao, Y. L. Xing, S. C. Zhang, *Electrochim. Acta*, 319 (2019) 359.
25. Z. Y. Luo, W. X. Lei, X. Wang, J. N. Pan, Y. Pan and S. Xia, *Electrochim. Acta*, 812 (2020) 152132.
26. W. Zhang, J. F. Zhang, Y. Zhao and X. Wang, *Mater. Lett.*, 255 (2019) 126595.
27. S. P. Li, X. Chen, F. Hu, R. Zeng, Y. H. Huang, L. X. Yuan and J. Xie, *Electrochim. Acta*, 304 (2019) 11.
28. S. S. Yao, H. Tang, M. Q. Liu, L. L. Chen, M. X. Jing, X. Q. Shen, T. B. Li and J. L. Tan, J. Alloy Compd., 788 (2019) 639.
29. Y. Y. Liang, N. P. Deng, J. G. Ju, X. H. Zhou, J. Yan, C. L. Zhong, W. M. Kang and B. W. Cheng, *Electrochim. Acta*, 281 (2018) 257.
30. W. M. Kang, L. L. Fan, N. P. Deng, H. J. Zhao, Q. X. Li, J. Yan and B. W. Cheng, *Chem. Eng. J.*, 333 (2018) 185.
31. X. Y. Li, N. Q. Fu, J. Z. Zou, X. R. Zeng, Y. M. Chen, L. M. Zhou and H. T. Huang, *Mater. Lett.*, 209 (2017) 505.
32. X. H. Zhao, M. Kim, Y. Liu, H. J. Ahn, K. W. Kim, K. K. Cho and J. H. Ahn, *Carbon*, 128 (2018) 138.
33. Q. Li, Z. A. Zhang, K. Zhang, J. Fang, Y. Q. Lai and J. Li, *J. Power Sources*, 256 (2014) 137.